PHYSICAL REVIEW B VOLUME 26, NUMBER 6 15 SEPTEMBER 1982

Eu^{2+} as an optical probe to follow precipitation processes in the system NaCl-$SrCl_2$

J. García-Solé, M. Aguilar G., and F. Agulló-López
Departamento de Optica y Estructura de la Materia, Universidad Autónoma de Madrid, Madrid, Spain

H. Murrieta S. and J. Rubio O.
Instituto de Física, Universidad Autonoma de Mexico, P. O. Box 20-364, Delegación Alvaro Obregón, 01000 México, D. F., México

The optical properties (absorption and luminescence) of a small concentration of divalent europium (6 mol ppm) incorporated into single crystals of NaCl doped with a higher concentration of divalent strontium (860 mol ppm) have been systematically investigated as a function of different annealing treatments in order to follow strontium precipitation in the NaCl matrix. The results indicate that the Eu^{2+} ions become incorporated into the Sr precipitates. The annealing of quenched samples in the range of temperatures (100–300 °C) produces the growth of three emission bands peaking at 450, 415, and 407 nm. The former two bands appear to be associated with metastable strontium precipitates from which grows the stable dihalide phase $SrCl_2$, responsible for the emission at 407 nm. From the analysis of the excitation spectra of these emission bands it is inferred that the structures of the metastable precipitates are quite similar to that of $SrCl_2$. On the other hand, the aging at room temperature for long times produces another two Sr-second-phase precipitates responsible for the emission bands peaking at 410 and 448 nm, the structures of these precipitates being different to that of strontium chloride.

I. INTRODUCTION

It is well known that an isolated impurity-vacancy dipole is not the only possible complex which can be found in alkali-halide crystals doped with divalent-cation impurities. In fact, the impurity-vacancy dipoles undergo aggregation leading to the formation of clusters of two or more dipoles which develop into one or various kinds of precipitates in the crystalline matrix. In the last few years, a lot of work has been performed dealing with this phenomenon in the alkali halides since many of the physical properties of these crystals, such as ionic conductivity,[1,2] mechanical strength,[3,4] radiation-induced coloring,[5,6] etc., may be considerably influenced by the presence of aggregates and impurity precipitates in the sample analyzed. The structure of these precipitates has been usually studied by x-ray diffraction,[7,8] electron microscopy,[9] and more recently by Raman spectroscopy.[10]

On the other hand, for the particular case of Pb^{2+} and Eu^{2+} as impurities in the alkali halides, the presence of precipitates in the crystal has been directly established from the analysis of the absorption and emission spectra since they have been reported to be quite dependent on the aggregation-precipitation state of these ions in the alkali-halide matrix.[11–13] This fact is quite relevant since meaningful studies dealing with the influence on the physical properties of the crystal of impurity aggregates, as well as of second-phase precipitates can then be performed taking advantage of the fact that additional information regarding the state of the impurity in the crystal may be obtained at any time. Unfortunately, for other divalent-cation impurities such as Sr^{2+}, Mn^{2+}, Ba^{2+}, Mg^{2+}, Cd^{2+}, etc., the presence of precipitates in the samples cannot be directly obtained from optical measurements. Therefore, more sophisticated techniques, which might not be used as routinely as the optical ones, are needed in order to get additional information on the precipitation state of the impurity in the crystal. This difficulty, however, may be avoided using as a probe another impurity ion which could be incorporated into the aggregates and precipitates formed modifying its optical spectra due to changes in the local crystalline environment. The potentiality of this technique has been recently tested by García-Solé *et al.*[14,15] who ar-

rived at the conclusion that the Pb^{2+} ion is a quite good optical probe to follow the clustering processes occurring in the NaCl crystal doped with different divalent-cation impurities such as Cd^{2+}, Ca^{2+}, and Sr^{2+}.

In this paper a detailed study dealing with the precipitation of Sr^{2+} ions in the NaCl matrix monitored using divalent europium as an optical probe is reported. The results show that at least two advantages can be obtained by using Eu^{2+} instead of lead to investigate strontium-precipitation in NaCl: (1) It is possible to get more information regarding the structures of the different second-phase precipitates by measuring the magnitude of the crystal-field splitting of the $4f^6 5d$ configuration of the Eu^{2+} ions when they are located inside them. These values can be calculated from the excitation spectra of the emission bands associated with the different precipitated phases. (2) The fluorescence measurements can be well performed at room temperature at which the emission spectrum of Pb^{2+} is strongly quenched.

II. EXPERIMENTAL

Single crystals of NaCl doubly doped with Sr^{2+} and Eu^{2+} were grown from the melt by the Czochralski method under a controlled atmosphere of dry argon, the crystals being slowly cooled to room temperature in the furnace. The dopants were $SrCl_2$ and $EuCl_2$, the latter being previously reduced from $EuCl_3 \cdot 6H_20$ with the use of standard techniques.[16] The concentration of strontium in the crystals employed was determined by atomic absorption spectrophotometry and the result was 860 mol ppm. To determine the concentration of divalent europium, optical-absorption measurements were performed in the doped samples following the same procedure as the one described elsewhere.[17] The result was 6 mol ppm. Thermal quenching was performed by heating the samples at 550 °C for ~30 min and then dropping them onto a copper block at room temperature (20 °C).

Optical-absorption measurements were made at room temperature with a Perkin-Elmer model 330 double-beam-recording spectrophotometer. The emission spectra were also obtained at room temperature with a Perkin-Elmer model 650-10S fluorescence-spectrophotometer with a resolution of ~ 2 nm in all cases. The excitation source was a 150-W xenon lamp which was calibrated for intensity versus wavelength and the excitation spectra have been corrected for this effect. All the emission spectra reported below were obtained using an excitation wavelength of 350 nm.

III. RESULTS

A. Optical-absorption spectra

Different spectra have been observed in the doubly doped samples depending upon the thermal treatment to which they were subjected. Figure 1 shows the optical-absorption spectra corresponding to a freshly quenched sample (I), a crystal aged at room temperature for 300 h (II), a sample annealed at 200 °C for 250 h [III(a)], and the one taken on a crystal which was cleaved from the "as-grown" boule [III(b)]. In all cases, the absorption spectrum consists of two structured broad bands which have been ascribed to transitions from the $4f^7$ ($^8S_{7/2}$) ground state of the Eu^{2+} ion to states in the $4f^6 5d$ configuration.[18] The separation between these two bands is a measure of the crystal-field splitting ($10Dq$) of the $5d$ orbital into its t_{2g} and e_g components. The structure of both bands has been interpreted as due to spin-orbit, Coulomb, and exchange interactions between the $5d$ and $4f$ electrons.[18] It is worthwhile to note that spectra II, III(a), and III(b) present an increasing background

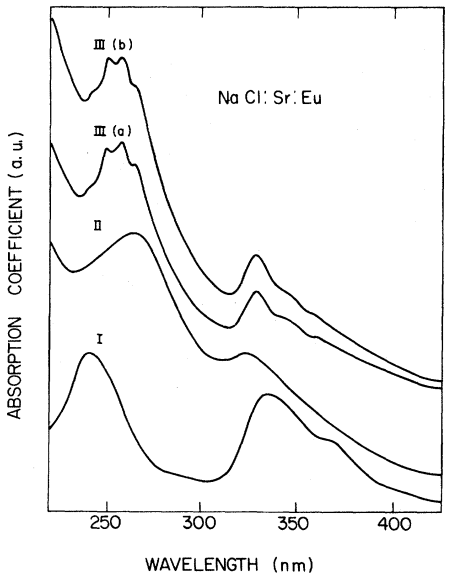

FIG. 1. Room-temperature optical-absorption spectra of Eu^{2+} in NaCl doubly doped with europium and strontium for a freshly quenched sample (I), a crystal aged at room temperature for 300 h (II), a sample annealed at 200 °C for 250 h [III(a)], and an "as-grown" sample [III(b)].

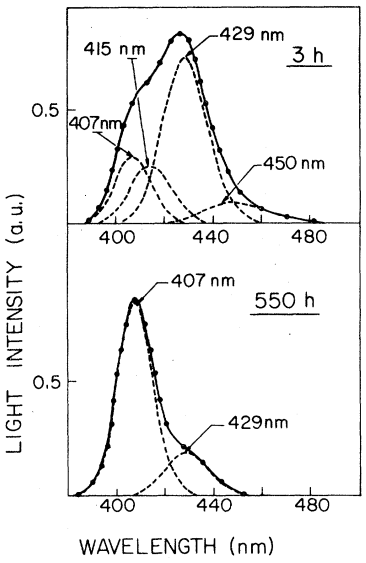

FIG. 2. Emission spectra of Eu^{2+} in doubly doped samples which has been annealed for 3 and 550 h at 280 °C, after a fast quench. The points represent the fit to the emission spectra using symmetric Gaussian-shape bands.

towards short wavelengths which may be the result of light scattering produced by strontium precipitates present in the samples.

B. Luminescence spectra

Immediately after quenching, the emission spectrum consists of only one symmetric Gaussian-shape band peaking at 429 nm and with a half-width of 0.14 eV.

Figure 2 shows the emission spectra obtained from a crystal which has been annealed at 280 °C for 3 and 550 h after the quenching treatment. The emission spectrum at the shorter time consists of four bands peaking at 407, 415, 429, and 450 nm, while after 550 h have elapsed, the spectrum consists mainly of the emission bands at 407 and 429 nm, the intensity of the latter band being considerably smaller than that of the former. Values for the half-width of each of these bands are given in Table I. In order to obtain all this information, the structured emission spectrum was decomposed into several symmetric Gaussian-shape bands, the number of which were initially determined by observing the shape of the contour. Then, a computer program was employed to change the peak position, intensity, bandwidth, and the possible number of the emission bands until a good fit (within 5%) to the experimental spectra was achieved. Figure 2 shows an example of this fit using the parameters given in Table I, as well as the decomposition of the emission spectra into the different Gaussian-shape bands. At this point, it should be pointed out that no attempt was made to perform the analysis mentioned above using asymmetric Gaussian-shape bands. The reason for the latter being that in those cases in which the experimental emission spectrum could be clearly decomposed into a small number of bands [as the one displayed in Fig. 2(b)], it was ascertained that the bands involved symmetric Gaussian shapes. On the other hand, a clear indication that asymmetric Gaussian-shape bands should be involved in the curve analysis was not found in any of the curves which were decomposed. Moreover, a good consistency was achieved using symmetric Gaussian-shape bands in the analysis performed of the different annealing treatments.

TABLE I. Peak position and bandwidth of the different bands observed in the the emission spectra of room- and high-temperature- (100, 200, 280 °C) annealed samples. Values for the $10Dq$ splitting measured from the excitation spectrum corresponding to each one of these emisssion bands are also given.

Sample	Peak position (nm)	Bandwidth (eV)	$10Dq$ (cm^{-1})	Reference
Quenched	429	0.14	12931	This work
Annealed at	407	0.13	10224	
high temperatures	415	0.14	10133	This work
	450	0.18	10012	
Annealed at	410	0.24	9743	
room temperature	416	0.14		This work
	448	0.28	10351	
$SrCl_2$:Eu^{2+}	410	0.14		Kobayasi *et al.*
$SrCl_2$:Eu^{2+}	409	0.13		Brixner and Ferretti

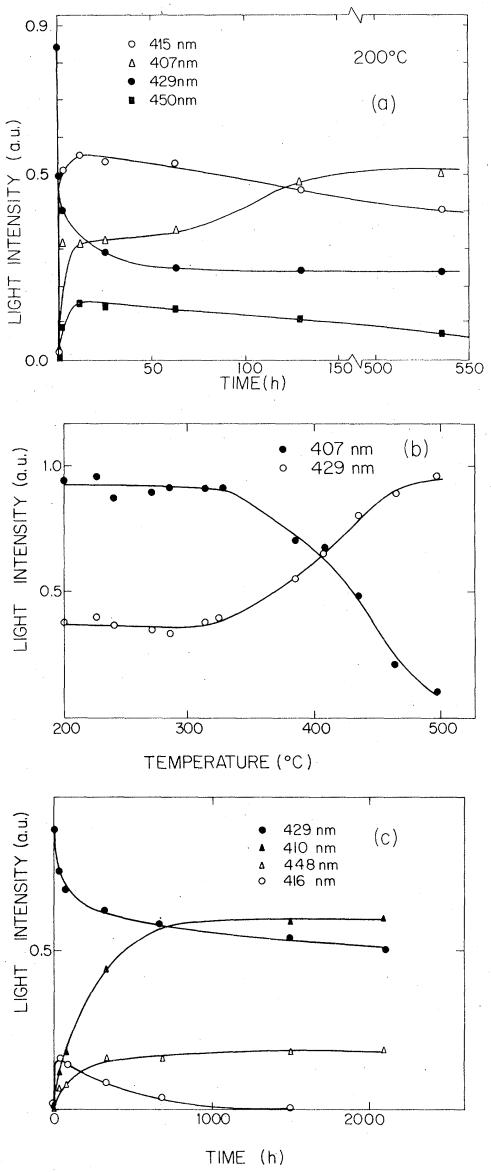

FIG. 3. (a) Evolution of the intensity of the emission bands peaking at 407, 415, 429, and 450 nm as a function of the annealing time at 200 °C. (b) Intensity of the emission bands peaking at 407 and 429 nm as a function of temperature. (c) Evolution of the intensity of the emission bands at 410, 416, 429, and 448 nm as a function of the time elapsed at room temperature after quenching.

The evolution of the emission spectrum was analyzed as a function of the annealing time at 100, 200, and 280 °C after the quenching treatment. The results are shown in Fig. 3(a) for samples annealed at 200 °C. To make these measurements the observed emission spectrum, at each time was decomposed following the procedure mentioned above. The aging at this temperature produces the growth of the emission bands peaking at 407, 415, and 450 nm up to ~10 h. As the annealing treatment proceeds, a saturation of the growth of these bands takes place. After ~65 h have elapsed the intensities of the emission bands at 450 and 415 nm begin to decay while that corresponding to the 407 nm band suffers a further increase up to ~450 h. During all this process, the intensity of the band peaking at 429 nm observed in the emission spectrum of the quenched samples decreases. The same qualitative behavior as that reported above was found when the samples were annealing at 100 and 280 °C. At the former temperature, however, the evolution is slower. On the other hand, at 280 °C the bands peaking at 415 and 450 nm disappeared after 50 and 130 h of annealing, respectively. Then, the emission spectrum consisted of only the 407- and 429-nm bands, the former being the prominent one. The thermal stability of the emission band peaking at 407 nm was also studied in the range of temperatures 25—600 °C in order to get additional information about the precipitated phase responsible for this emission. The results are shown in Fig. 3(b). To perform these measurements, the sample whose emission spectrum is displayed in Fig. 2(b), was heated for 30 min at the temperatures shown in the figure and then rapidly quenched to room temperature to record the fluorescence spectrum. As can be seen from this figure, the thermal dissolution of the Sr-second-phase precipitate responsible for the 407-nm band occurs in the range of temperatures 300—500 °C.

At variance with the results mentioned above, the aging at room temperature produced the growth of three emission bands peaking at 410, 416, and 448 nm which are different from those which develop during the annealing at high temperatures. In Fig. 3(c) the evolution of the intensities of these bands as a function of the time elapsed at room temperature after quenching is presented. These measurements show that the 448- and 410-nm bands grow in parallel, and both at the expense of the band peaking at 429 nm. On the other hand, the emission at 416 nm grows up to ~70 h. Then, its intensity decreases and it disappears after 1000 h of annealing. The bandwidths of these bands are also given in Table I. They were obtained by decomposing the observed emission spectrum following the same procedure as the one described above. It is important to note that several attempts were made to fit the experimental emission spectra observed in the room-temperature-annealed samples, using the same symmetric

Gaussian-shape bands than those employed to fit the emission spectra of those crystals which were aged in the range of temperatures 100–300 °C. However, all of them were unsuccessful. This fact indicated that the changes in the emission spectrum as a function of the annealing time at room temperature (RT) were due to the growth of three emissions bands (410, 416, and 448 nm) which are different from those which developed in the emission spectra of the high-temperature- (HT-) annealed crystals (407, 415, and 450 nm). Moreover, a comparison of the excitation spectra of the former emissions with those of the latter gave evidence of their different nature.

C. Excitation spectra

Figure 4 shows the excitation spectra for the bands peaking at 407 (HT-annealed crystals), 410, and 448 nm (RT-annealed crystals). The excitation spectra of the emission bands peaking at 415 and 450 nm (HT-annealed crystals) are quite similar to that of the 407-nm band and correlate quite well with the absorption spectra III(a) and III(b). Reference to Fig. 4 shows that the spectra of the 410- and 448-nm bands are quite different between them and also from that of the 407-nm band. This fact gives evidence of the different nature of the Sr-second-phase precipitates responsible for these emissions. The excitation spectrum of the 429-nm band, observed in the quenched samples, is also included in Fig. 4 for the sake of comparison. It correlates quite well with the absorption spectrum

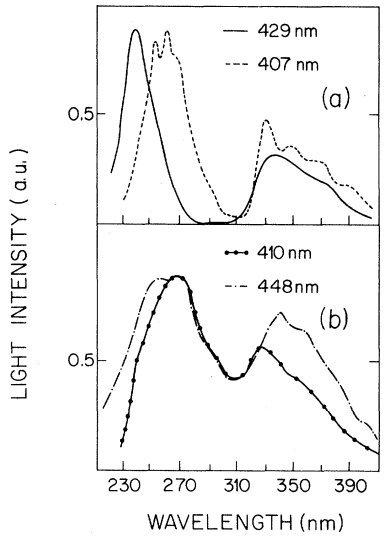

FIG. 4. Excitation spectra corresponding to the emission bands peaking at: (a) 407 nm (HT-annealed crystals) and 429 nm (quenched crystals); (b) 410 and 448 nm (RT-annealed crystals).

I. Values for the $10Dq$ splitting calculated from the centers of gravity of the two broad bands in the excitation spectrum corresponding to the fluorescence bands mentioned above are also reported in Table I.

IV. DISCUSSION

The data presented above strongly suggest that the europium ions are associated with strontium aggregates, as well as incorporated into the second-phase strontium precipitates.

The emission band peaking at 429 nm is very similar to that previously reported[13] in quenched samples of NaCl:Eu^{2+}, although its peak position is slightly shifted to longer wavelengths. Since this band is the only one observed after a fast quench from high temperatures, one is tempted to consider that in principle, the complexes responsible for this band are isolated Eu^{2+} cation-vacancy dipoles, as well as possible mixed Sr-Eu centers. The shift in the peak position of this band to longer wavelengths may be the result of a small difference between the crystal field acting on the Eu^{2+} site in the mixed complexes (12 931 cm^{-1}) and in that occupied by this ion when it is in the dipole state in the NaCl matrix (12 849 cm^{-1}).[13]

The data presented in Fig. 3(a) suggest that the precipitated phases responsible for the emission bands peaking at 415 and 450 nm are metastable ones from which grows the stable second-phase strontium precipitate responsible for the band peaking at 407 nm. The latter band is the prominent one in the spectrum of the annealed samples at 280 °C. At this temperature, it has been established that strontium precipitation into the stable dihalide phase $SrCl_2$ occurs, using x-ray diffraction techniques.[19] Also, at this temperature the maximum nucleation of $SrCl_2$ particles in the NaCl matrix has been reported by Andreev and Smirnov[20] using the flotation technique. It is suggested, therefore, that the emission band peaking at 407 nm is due to divalent europium ions embedded into the $SrCl_2$ precipitates. This conclusion can be supported by the following facts: (1) The peak position and bandwidth of the emission band previously reported[21,22] for Eu^{2+} in monocrystalline $SrCl_2$ are quite similar to those given in Table I for the 407-nm band, (2) EPR measurements performed in the annealed samples in which the 407-nm band was the prominent one revealed that Eu^{2+} ions are incorporated into the $SrCl_2$ precipitates substituting for the host cation Sr^{2+} ions,[23] and (3) the range of temperatures at which occurs the thermal dissolution of the precipitated phase

responsible for the 407-nm band [Fig. 3(b)] is quite similar to that previously reported for the dissolution of $SrCl_2$ precipitates in the NaCl matrix using a similar strontium concentration.[2] On the other hand, since the $10Dq$ splitting measured from the excitation spectra of the emission bands at 407, 415, and 450 nm are quite similar (Table I), it is concluded that the crystal field acting at the site occupied by the europium ion in each of the precipitated phases responsible for these bands is nearly identical. This result suggests that the structures of the second-phase precipitates associated with the latter two emissions might be quite similar to that of $SrCl_2$.

With regard to the strontium-precipitation processes which occur at room temperature, it appears that the precipitated phase associated with the emission band peaking at 416 nm is a metastable one from which grow those responsible for the emissions at 410 and 448 nm. The excitation spectra of the latter two emissions show that the crystal field at the Eu^{2+} site in the precipitated phases responsible for these bands is different, its value being smaller in the former. This fact suggests that the structures of these two strontium precipitates may be different. Additional information about the second-phase precipitate associated with the emission band peaking at 410 nm has been obtained from EPR measurements performed in those samples for which this emission was the prominent one.[23] It was ascertained that the Eu^{2+} ion occupies cubic-symmetry sites in this precipitate, the cubic crystal field acting on the impurity ion being smaller than in the case in which it was embedded into the $SrCl_2$ phase. Moreover, the crystal lattice of this precipitate was found to be parallel to that of NaCl. All these results indicate that the second-phase precipitate responsible for the band peaking at 410 nm possesses a cubic structure which appears to be different from that of $SrCl_2$. Also, the results given above indicate that the structure of the Sr-precipitated phase responsible for the emission band peaking at 448 nm is different from that of $SrCl_2$, as well as from that of the second-phase precipitate associated with the 410-nm band. Unfortunately, nothing can be said about the metastable-precipitated phase responsible for the emission at 416 nm in view of the fact that the excitation spectrum corresponding to this emission could not be clearly obtained. The reason for this is that some contamination of other excitation spectra corresponding to the emission bands peaking at 410 and 448 nm was always observed in the excitation spectrum of the 416-nm band. This fact did not allow us to measure the $10Dq$ splitting of this spectrum precisely, and therefore a reliable comparison with the other values was not possible.

Finally, we may conclude that the divalent europium ion has proven to be a quite useful optical probe to follow strontium precipitation in the NaCl matrix. Unfortunately, to our knowledge, systematic x-ray diffraction studies dealing with the nucleation processes of $SrCl_2$ precipitates in the NaCl matrix have not been performed up to date. It will be very interesting to perform these studies in order to determine the structures of the different strontium-precipitated phases associated with the emission bands presented above. This determination, along with those of this study, could give a complete picture of the precipitation processes of Sr^{2+} at room and high temperatures, allowing then to know the state of aggregation precipitation of the impurity in the matrix, at any time, from the data presented in this paper.

ACKNOWLEDGMENTS

This work was partially supported by CONACyT (México) and CSIC (Spain) under Contract No. ICAIESP 800666 and by the U. S. Air Force under Grant No. AFOSR-79-0115.

[1]N. Bonanos and E. Lilley, Solid State Ionics 1, 223 (1980).
[2]N. Brown and I. M. Hoodless, J. Phys. Chem. Solids 28, 2297 (1967).
[3]J. García-Solé, C. Zaldo, and F. Agulló-López, Philos. Mag. A 41, 177 (1980).
[4]E. Orozco M., A. Mendoza A., J. Soullard, and J. Rubio O., Jpn. J. Appl. Phys. 21, 249 (1982).
[5]C. Sánchez, I. S. Lerma, F. Jaque, and F. Agulló-López, Cryst. Lattice Defects 6, 227 (1976).
[6]J. L. Pascual and F. Agulló-López, Cryst. Lattice Defects 7, 161 (1977).
[7]K. Suzuki, J. Phys. Soc. Jpn. 13, 179 (1958).
[8]K. Suzuki, J. Phys. Soc. Jpn. 16, 67 (1961).
[9]M. Yacamán, L. W. Hobbo, and M. J. Goringe, Phys. Status Solidi A 39, K85 (1977).
[10]J. M. Calleja, A. Ruiz, F. Flores, V. R. Velasco, and E. Lilley, J. Phys. Chem. Solids. 41, 1367 (1980).
[11]J. L. Pascual, L. Arizmendi, F. Jaque, and F. Agulló-López, J. Lumin. 17, 325 (1978).
[12]L. Marculescu, Phys. Status. Solidi B 80, 265 (1977).
[13]F. J. López, H. Murrieta S., J. Hernández A., and J.

Rubio O., Phys. Rev. B 22, 6428 (1980).
[14]J. Garciá-Solé, C. Zaldo, and F. Agulló-López, J. Lumin. 24/25, 193 (1981).
[15]J. García-Solé, C. Zaldo, and F. Agulló-López, Phys. Rev.B 25, 3050 (1982).
[16]R. A. Cooley and D. M. Yost, Inorg. Synth. 2, 71 (1946).
[17]J. Hernández A., W. K. Cory, and J. Rubio O., Jpn. J. Appl. Phys. 18, 533 (1979).
[18]J. Hernández A., W. K. Cory, and J. Rubio O., J. Chem. Phys. 72, 198 (1980).
[19]E. Laredo and E. Dartyge, Acta Crystallogr. Sect. A 27, 353 (1971).
[20]G. A. Andreev and B. I. Smirnov, Phys. Status. Solidi (A) 15, 207 (1973).
[21]T. Kobayasi, S. Mtoczkowski, J. F. Owen, and L. H. Brixner, J. Lumin. 21, 247 (1980).
[22]L. H. Brixner and A. Ferretti, J. Solid State Chem. 18, 111 (1976).
[23]H. Murrieta, F. J. López, J. García-Solé, M. Aguilar, and J. Rubio O., J. Chem. Phys. 77, 189 (1982).